

Synthesis and Structure–Activity Relationship Studies in Translocator Protein Ligands Based on a Pyrazolo[3,4-*b*]quinoline Scaffold

Andrea Cappelli,^{*,†} Giulia Bini,[†] Salvatore Valenti,[†] Germano Giuliani,[†] Marco Paolino,[†] Maurizio Anzini,[†] Salvatore Vomero,[†] Gianluca Giorgi,[‡] Antonio Giordani,[§] Luigi Piero Stasi,[§] Francesco Makovec,[§] Carla Ghelardini,^{||} Lorenzo Di Cesare Mannelli,^{||} Alessandra Concas,[⊥] Patrizia Porcu,[⊥] and Giovanni Biggio[⊥]

[†]Dipartimento Farmaco Chimico Tecnologico and European Research Centre for Drug Discovery and Development, Università degli Studi di Siena, Via A. Moro, 53100 Siena, Italy

[‡]Dipartimento di Chimica, Università degli Studi di Siena, Via A. Moro, 53100 Siena, Italy

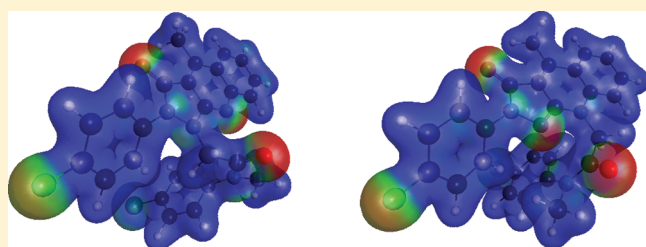
[§]Rottapharm SpA, Via Valosa di Sopra 7, 20052 Monza, Italy

^{||}Dipartimento di Farmacologia Preclinica e Clinica “M. Aiazzi Mancini”, Università degli Studi di Firenze, Viale G. Pieraccini 6, 50139 Firenze, Italy

[⊥]Dipartimento di Biologia Sperimentale “B. Loddo”, Università degli Studi di Cagliari, Cittadella Universitaria, SS 554 (km 4.500), 09042 Monserrato (Cagliari), Italy

Supporting Information

ABSTRACT: As a further development of our large program focused on the medicinal chemistry of translocator protein [TSPO (18 kDa)] ligands, a new class of compounds related to alpidem has been designed using SSR180575, emapunil, and previously published pyrrolo[3,4-*b*]quinoline derivatives **9** as templates. The designed compounds were synthesized by alkylation of the easily accessible 4-methyl-2-phenyl-1*H*-pyrazolo[3,4-*b*]quinolin-3(2*H*)-one derivatives **13–15** with the required bromoacetamides. Along with the expected 2-(4-methyl-3-oxo-2-phenyl-2,3-dihydro-1*H*-pyrazolo[3,4-*b*]quinolin-1-yl)acetamide derivatives **10**, 2-(4-methyl-3-oxo-2-phenyl-2*H*-pyrazolo[3,4-*b*]quinolin-9(3*H*)-yl)acetamide isomers **11** were isolated and characterized. The high TSPO affinity shown by new pyrazolo[3,4-*b*]quinoline derivatives **10** and especially **11** leads the way to further expand the chemical diversity in TSPO ligands and provides new templates and structure–affinity relationship data potentially useful in the design of new anxiolytic and neuroprotective agents.



■ INTRODUCTION

The peripheral benzodiazepine receptor (PBR) is a protein of 18 kDa showing five transmembrane domains, pharmacologically distinct from the central benzodiazepine receptor (CBR), originally discovered in the periphery as an alternative binding site of diazepam, and recently renamed “translocator protein (18 kDa)” (TSPO).¹ TSPO is primarily localized at the outer mitochondrial membrane, in particular, at the outer/inner mitochondrial membrane contact sites,² but it is also localized at the nucleus and the perinuclear region in breast cancer cells³ as well as at the plasma membrane of erythrocytes.⁴ TSPO interacts with various other proteins, including the 32 kDa voltage-dependent anion channel (VDAC) and the 30 kDa adenine nucleotide transporter (ANT), which are components of the mitochondrial permeability transition pore (MPTP).

Although the exact physiological role of TSPO is not yet completely defined, evidence has been collected about its involvement in cholesterol transport across the mitochondrial membrane, regulation of steroid biosynthesis, mitochondrial respiration,

MPTP opening, and apoptosis as well as cell proliferation and differentiation. It has been suggested that TSPO functions are related to various aspects of the host-defense response.⁵

TSPO can be found in the whole body: glandular and secretory tissues are particularly rich in TSPO, but it is also present in renal and myocardial tissue, as well as in hemopoietic and lymphatic cells. Low levels of TSPO are expressed in liver and brain, where it is limited to glial cells (astrocytes and microglia). A dramatic increase in TSPO density occurs in glial cells in response to brain injury or inflammation as well as following a number of neuropathological conditions.⁶ These include gliomas, stroke, herpes and HIV encephalitis, and neurodegenerative disorders such as Alzheimer's disease, multiple sclerosis, amyotrophic lateral sclerosis, Parkinson's disease, and Huntington's disease. Moreover, changes in TSPO expression levels have been observed in patients suffering from generalized and separation anxiety, panic attacks,

Received: June 14, 2011

Published: September 14, 2011

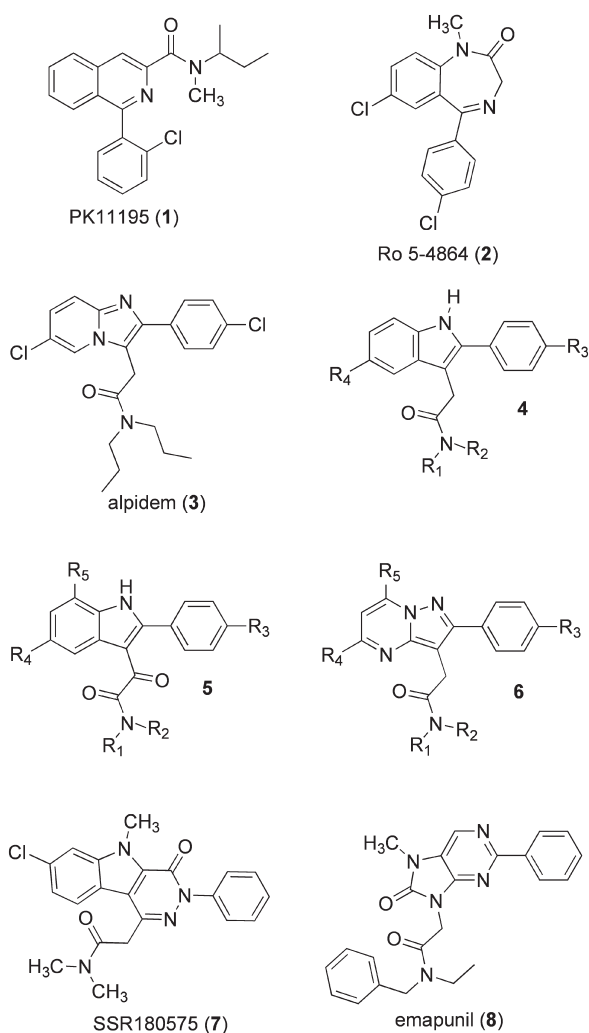


Figure 1. Structure of some relevant TSPO ligands.

post-traumatic stress, and obsessive—compulsive disorders.⁷ Therefore, TSPO can be exploited as a diagnostic marker to follow disease progression and therapy efficacy by means of the biomedical imaging technique PET (positron emission tomography) but also as a therapeutic target.

In addition to classical synthetic TSPO ligands PK11195 (1, Figure 1) and Ro5-4864 (2), several other chemically different ligands have been developed, especially in the family of molecules related to alpidem (3). Among them, indoleacetamides 4,⁸ indolylglyoxylamides 5,⁹ pyrazolopyrimidine derivatives 6,¹⁰ and SSR180575¹¹ (7, Figure 1) stimulate the biosynthesis of pregnenolone metabolites acting as positive allosteric modulators of GABA neurotransmission. Thus, TSPO ligands capable of stimulating neurosteroid biosynthesis can represent promising candidates for fast-acting anxiolytic agents lacking the unwanted benzodiazepine-like side effects. For instance, emapunil (AC5216, XBD-173, 8) enhances GABA-mediated neurotransmission and exerts antipanic activity in humans without causing sedation or withdrawal symptoms.¹² On the other hand, 7 was reported to promote neuronal survival and repair in axotomy and neuropathy models and is potentially useful in the treatment of neurodegenerative diseases. The increase in pregnenolone accumulation in the brain and sciatic nerve suggests that the neuroprotective effects shown by 7 are steroid-mediated.¹¹

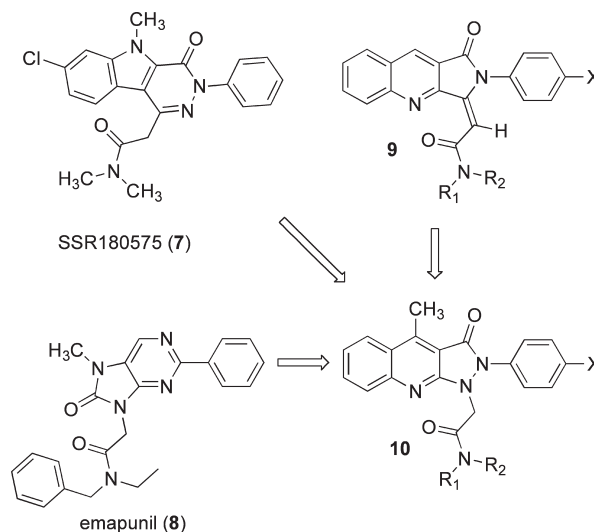


Figure 2. Design of TSPO ligands 10.

Our interest in the design and synthesis of TSPO ligands led to development of potent compounds 9 structurally related to alpidem.¹³ Thus, in the progress of our large program focused on the medicinal chemistry of TSPO ligands, pyrazolo[3,4-*b*]-quinoline derivatives 9, pyridazino[4,5-*b*]indole-1-acetamide 7, and emapunil (8) were considered as structural templates in the design of new tricyclic derivatives 10 (Figure 2).

In particular, the pyrazolo[3,4-*b*]quinoline tricyclic system of compounds 9 was transformed into the pyrazolo[3,4-*b*]quinoline ring system of compounds 10 that can be considered as a structural hybrid between the pyridazino[4,5-*b*]indole moiety of 7 and the pyrazolo[3,4-*b*]quinoline system of compounds 9. Moreover, the rigid ylidenacetamide moiety of compounds 9 was converted into an acetamide side chain attached to the heteroaromatic system through a heterocyclic nitrogen atom as was the case with emapunil. This paper describes the synthesis and the preliminary pharmacological (in vitro and in vivo) characterization of TSPO ligands 10 based on the pyrazolo[3,4-*b*]quinoline scaffold and the serendipitous discovery of isomers 11 with subnanomolar TSPO affinity.

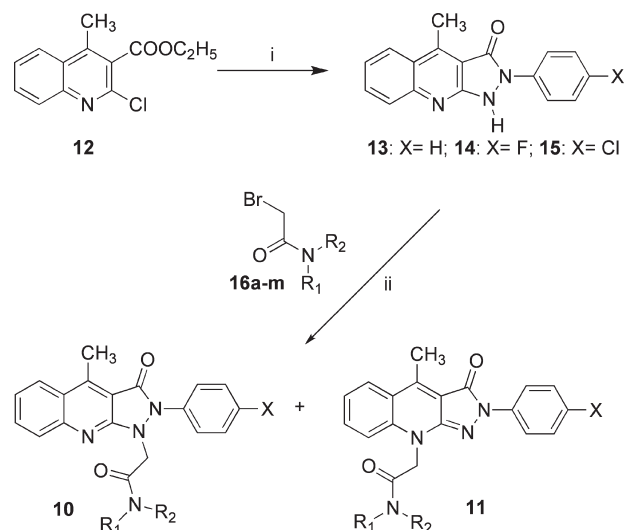
RESULTS

Chemistry. Target pyrazolo[3,4-*b*]quinoline derivatives 10 were synthesized as depicted in Scheme 1.

Reaction of 2-chloroquinoline derivative 12¹⁴ with the suitable phenylhydrazines gave the corresponding tricyclic compounds 13–15 as dark-red crystalline solids. The structure of compound 13 was characterized by crystallographic studies (Figure 3).

Compounds 13–15 were alkylated in the presence of sodium carbonate with the required bromoacetamide derivatives 16a–m (see Supporting Information) to obtain substantial amounts of alkylation products 10 (yellow crystals) along with small amounts of intensely dark-red-colored compounds 11. In some instances the purification of compounds 11 proved to be difficult. However, compounds 11a,b,e,g,n,q were isolated in acceptable yield (6–30%) and good purity after repeated chromatographic purifications and subsequent recrystallization and were appropriately characterized.

The structure of some representative target pyrazolo[3,4-*b*]quinoline derivatives (10b,e,h,q,r,t) was studied by crystallography, which confirmed that (in the experimental conditions) the

Scheme 1. Synthesis of Target Compounds 10 and 11^a

^a Reagents: (i) C₆H₄NHNH₂, 1-pentanol, (or X-C₆H₄NHNH₂·HCl, Na₂CO₃, 1-pentanol); (ii) Na₂CO₃, DMF.

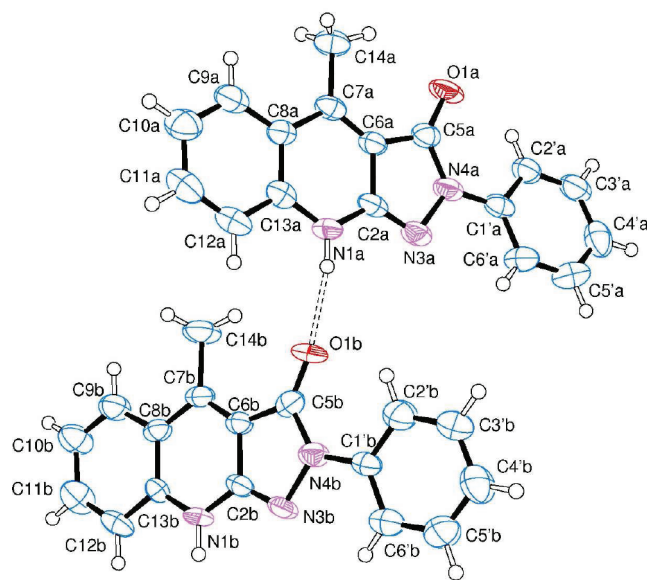


Figure 3. Structure of compound 13 asymmetric unit found by crystallography. Ellipsoids enclose 50% probability.

preferred alkylation site is the free pyrazole nitrogen and it shows for this atom a pyramidal character in all the compounds studied (Figure 4).

Mass spectrometry confirmed that compounds **11a,b,e,g,n,q** are isomers of compounds **10a,b,e,g,n,q**, and the comparison of NOESY spectrum of compound **11b** with that of its isomer **10b** showed that the acetamide methylene of the former is in dipolar contact with H-8, while in the latter a weak cross peak was observed between H-2'/6' and acetic CH₂ protons (Figure 5). The NMR studies performed with the couple **10b/11b** led to the hypothesis that the freely rotating aromatic ring (FRA)¹³ of compound **11b** is at least partially constrained in a coplanar position with respect to the tricyclic system. This hypothesis is supported by the difference in the chemical shift observed for the

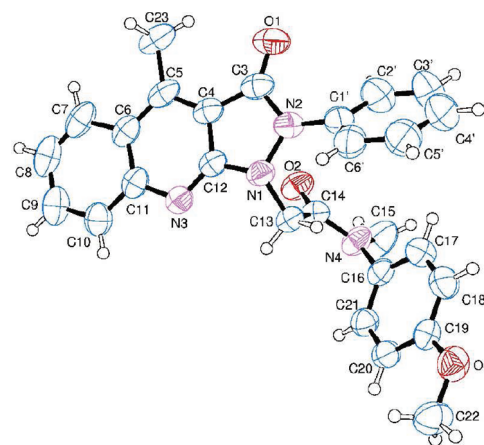


Figure 4. Crystallographic structure of compound **10h**. Ellipsoids enclose 50% probability.

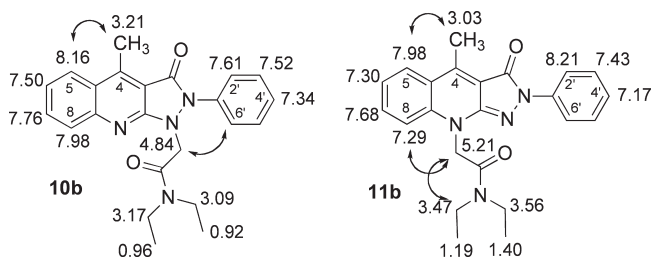


Figure 5. Comparison of the ¹H NMR features of compounds **10b** and **11b**. The spectra were performed at 400 MHz in CDCl₃ at room temperature, and the chemical shift values are expressed in ppm. The double arrows indicate significant NOESY contacts.

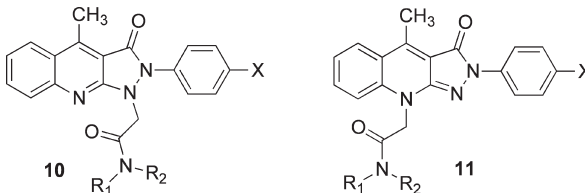
signals attributed to H-2'/6' in the couple **10b/11b**. In compound **10b**, the proximity between acetamide substituent and FRA leads the phenyl substituent to adopt an orientation almost perpendicular with respect to the plane of the tricyclic system (Figure 4) and the signal attributed to H-2'/6' resonates at 7.61 ppm. On the other hand, the phenyl substituent of compound **11b** can be considered a true freely rotating aromatic ring when potential nonconventional H-bonds are neglected. However, the low-field chemical shift (8.21 ppm, Figure 5) of the signal attributed to H-2'/6' of **11b** suggests that the FRA of this compound spends a significant time in the coplanar conformation.

In Vitro Binding Studies. Compounds **10a–t** and **11a,b,e,g,n,q** were tested for their potential activity in inhibiting the specific binding of [³H]**1** to rat cerebral cortex membranes in comparison with unlabeled **1**, and the results of the binding studies are shown in Table 1. The compounds tested show TSPO affinities in the micromolar to the subnanomolar range with a modulation suitable for structure–affinity relationship analysis.

In particular, the most striking result is that compounds **11** are very potent TSPO ligands showing subnanomolar IC₅₀ values, whereas the corresponding isomers **10** are around 1–2 orders of magnitude less potent. The difference suggests a better spatial arrangement for the acetamide side chain with respect to the planar aromatic region (PAR)¹³ in compounds **11** with respect to compounds **10** (Figure 6).

It is noteworthy that the structure–affinity relationships are quite similar in the two different series of isomers **10a,b,e,g** and

Table 1. TSPO Binding Affinities of Compounds 10 and 11



| compd | R ₁ | R ₂ | X | IC ₅₀ (nM) ± SEM ^a |
|---------|--|--|----|--|
| 10a | —CH ₃ | —(CH ₂) ₃ CH ₃ | H | 65 ± 10 |
| 10b | —C ₂ H ₅ | —C ₂ H ₅ | H | 180 ± 27 |
| 10c | —CH(CH ₃) ₂ | —CH(CH ₃) ₂ | H | 1392 ± 153 |
| 10d | —(CH ₂) ₂ CH ₃ | —(CH ₂) ₂ CH ₃ | H | 90 ± 9.9 |
| 10e | —(CH ₂) ₃ CH ₃ | —(CH ₂) ₃ CH ₃ | H | 152 ± 21 |
| 10f | —CH ₃ | —C ₆ H ₅ | H | 117 ± 7.0 |
| 10g | —CH ₃ | <i>p</i> -Cl-C ₆ H ₄ — | H | 1.8 ± 0.24 |
| 10h | —CH ₃ | <i>p</i> -CH ₃ OC ₆ H ₄ — | H | 17 ± 1.6 |
| 10i | —CH ₃ | —CH ₂ C ₆ H ₅ | H | 881 ± 70 |
| 10j | —CH ₂ C ₆ H ₅ | —C ₂ H ₅ | H | 220 ± 37 |
| 10k | —CH ₂ C ₆ H ₅ | —CH(CH ₃) ₂ | H | 304 ± 36 |
| 10l | —CH ₂ C ₆ H ₅ | —(CH ₂) ₃ CH ₃ | H | 697 ± 91 |
| 10m | —CH ₂ C ₆ H ₅ | —CH ₂ C ₆ H ₅ | H | 3464 ± 416 |
| 10n | —CH ₃ | —(CH ₂) ₃ CH ₃ | F | 110 ± 14 |
| 10o | —C ₂ H ₅ | —C ₂ H ₅ | F | 2271 ± 204 |
| 10p | —(CH ₂) ₂ CH ₃ | —(CH ₂) ₂ CH ₃ | F | 87 ± 6.1 |
| 10q | —CH ₃ | <i>p</i> -Cl-C ₆ H ₄ — | F | 6.8 ± 0.81 |
| 10r | —CH ₃ | —(CH ₂) ₃ CH ₃ | Cl | 144 ± 23 |
| 10s | —(CH ₂) ₂ CH ₃ | —(CH ₂) ₂ CH ₃ | Cl | 90 ± 8.1 |
| 10t | —CH ₃ | <i>p</i> -Cl-C ₆ H ₄ — | Cl | 16 ± 1.3 |
| 11a | —CH ₃ | —(CH ₂) ₃ CH ₃ | H | 0.14 ± 0.002 |
| 11b | —C ₂ H ₅ | —C ₂ H ₅ | H | 0.83 ± 0.074 |
| 11e | —(CH ₂) ₃ CH ₃ | —(CH ₂) ₃ CH ₃ | H | 0.34 ± 0.049 |
| 11g | —CH ₃ | <i>p</i> -Cl-C ₆ H ₄ — | H | 0.13 ± 0.067 |
| 11n | —CH ₃ | —(CH ₂) ₃ CH ₃ | F | 0.13 ± 0.016 |
| 11q | —CH ₃ | <i>p</i> -Cl-C ₆ H ₄ — | F | 0.28 ± 0.064 |
| PK11195 | | | | 1.3 ± 0.15 |

^a Each value is the mean ± SEM of 3 independent determinations performed in duplicate and represents the concentration giving half the maximum inhibition of [³H]1 (final concentration 1.0 nM) specific binding to rat cerebral cortex membranes.

11a,b,e,g. As a matter of fact, *N*-methyl-*p*-chloroacetanilide derivatives **10g** and **11g** are the most potent ligands of the respective series and the affinity is lower in the compounds bearing two *n*-butyl substituents (**10e** and **11e**) or two ethyl substituents (**10b** and **11b**). However, in the subseries of compounds **10b,e,g**, the affinity modulation is more dramatic, with variations of 2 orders of magnitude, while in the subseries **11b,e,g**, the affinity variations are within 1 order of magnitude. Moreover, in the series of compounds **10**, the replacement of *p*-chlorophenyl substituent with a *n*-butyl one produces a significant decrease in TSPO affinity (compare **10a** vs **10g**), while *N*-methyl-*N*-butylacetamide derivative **11a** and *N*-methyl-*p*-chloroacetanilide derivatives **11g** are equipotent. These results suggest the existence of both analogies and differences in the interaction of compounds **10** and **11** with TSPO recognition site. In general, the structure–affinity relationship analysis in the series

of compounds **10** shows a complex trend in which the above-cited dramatic effects coexist with a subtle affinity modulation resulting from significant structural changes. As a matter of fact, some compounds **10** with different substituents display very similar affinities in the submicromolar range (e.g., **10b,e,f,j,k**). The most significant structure–affinity relationships concern the negative effect of the presence of branched substituents in compound **10c** (compare **10c** with **10d**) and of the benzyl substituent in **10i** (compare **10i** with **10a**). These negative effects are less significant when a single branched substituent is present, as it occurs in compound **10k** (compare **10k** with **10j**), and when the benzyl substituent is combined with a small alkyl substituent. In fact, benzyl derivatives **10j,k,l** show TSPO affinities higher with respect to both dibenzyl derivative **10m** and *N*-methylbenzyl congener **10i**. Finally, the presence of a fluorine atom in the freely rotating aromatic ring (FRA) is tolerated in *N*-methyl-*p*-chloroacetanilide derivatives **10q**, **11q**, and *N*-methyl-*N*-butylacetamide derivative **11n**.

In Vivo Studies. On the basis of the intriguing results described for emapunil and pyridazino[4,5-*b*]indole-1-acetamide **7**,^{11,12} some compounds showing TSPO affinities in the nanomolar range were selected for a suitable in vivo pharmacological characterization in anxiety and neuropathy animal models.

Thus, the potential antianxiety activity of compounds **10g,q,t** and **11a** was evaluated in mice by means of the light/dark box test. In this experimental paradigm, the activity of the test compounds is indicated by the increase in the time spent in the aversive compartment (illuminated area) with respect to that spent in the dark. Compound **10t**, at oral doses of 3.0 and 10 mg/kg, increased significantly the time spent in the aversive compartment (Table 2).

Similar results were obtained with emapunil at the same doses, but some discrepancies were observed with respect to the results described in the literature for this reference compound, which was reported to show significant effects at oral doses of 0.003 and 0.01 mg/kg.^{12b} The other reference compound used in this test, diazepam at an oral dose of 1.0 mg/kg, produced an effect very similar to that shown by **10t** at the maximal dose tested (10 mg/kg). These results for compound **10t** indicate its potential utility for the treatment of anxiety disorders. On the other hand, compound **11a** was significantly active only at the maximal dose (10 mg/kg) and the remaining compounds **10g,q** were inactive even at 30 mg/kg po. These results demonstrate that very minor structural modifications may alter the physicochemical features responsible for the pharmacokinetic and in vivo pharmacological properties without altering the binding to the receptor. In fact, the variation of the atom in para-position of FRA in the series of compounds **10g,q,t** produces significant changes in the in vivo activity different from those observed in the in vitro binding to TSPO.

It is noteworthy that compound **10t** was found to be more active than its analogues **10g,q** also in a rat model of mono-neuropathy (Table 3). In fact, compound **10t**, at oral doses of 5.0 and 50 mg/kg, decreased the paw pressure significantly, while **10g,q** showed significant effects only at the highest dose tested (50 mg/kg). The duration of the action of the compounds was rather short because after 45 min from the administration a significant effect was observed only for *p*-chloroderivative **10t** at the highest oral dose of 50 mg/kg.

CONCLUSION

The straightforward synthesis and the high TSPO affinity shown by new pyrazolo[3,4-*b*]quinoline derivatives **10** and especially **11**

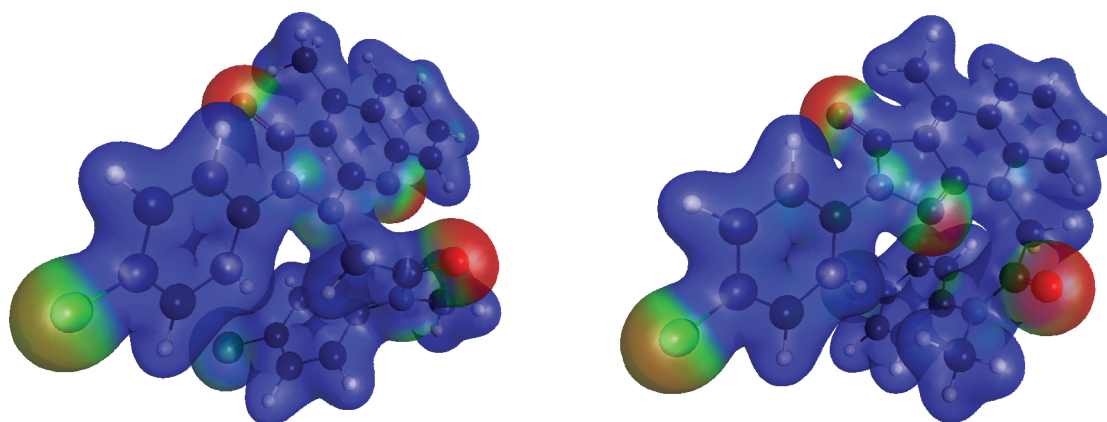


Figure 6. Comparison between the electrostatic potentials mapped on the electron density surface of isomers **10q** (left, $IC_{50} = 6.8$ nM) and **11q** (right, $IC_{50} = 0.28$ nM). The calculations were performed at Hartree–Fock level of theory and using 6-31G* as basis set. The scale of the electrostatic potential is negative (red) to positive (blue). The difference in TSPO affinity between compounds **10** and **11** is probably related to the spatial arrangement of the amide carbonyl playing a key role in the interaction with TSPO.

Table 2. Effect of Compounds **10g,q,t**, **11a**, Emapunil, and Diazepam in the Light/Dark Box Test^a

| compd | dose (mg/kg) po | time in light box (s) |
|------------|-----------------|-----------------------|
| 10g | 3 | 103.8 ± 7.1 |
| | 10 | 112.3 ± 8.0 |
| | 30 | 107.6 ± 7.7 |
| 10q | 3 | 106.8 ± 9.3 |
| | 10 | 117.5 ± 8.7 |
| | 30 | 111.3 ± 7.1 |
| 10t | 1 | 108.9 ± 8.3 |
| | 3 | 135.2 ± 7.6* |
| | 10 | 169.0 ± 6.4* |
| 11a | 1 | 103.7 ± 7.4 |
| | 3 | 117.4 ± 9.2 |
| | 10 | 151.5 ± 8.1* |
| emapunil | 1 | 110.8 ± 6.9 |
| | 3 | 137.3 ± 8.6^ |
| | 10 | 162.3 ± 7.7* |
| diazepam | 1 | 171.6 ± 9.3* |
| vehicle | | 116.4 ± 7.5 |

^a All drugs were administered 30 min before the test. Each value is the mean ± SEM of at least 8 mice per group. ^P < 0.05; *P < 0.01 versus vehicle-treated mice.

leads the way to further expand the chemical diversity in TSPO ligands and provides new templates and structure–affinity relationship data for the design of new TSPO modulators. Moreover, the oral activity of compound **10t** in both the light/dark box test and in a model of mononeuropathy offers additional evidence of the potential role of TSPO as a therapeutic target.

EXPERIMENTAL SECTION

Chemistry. All chemicals used were of reagent grade. Yields refer to purified products and are not optimized. Melting points were determined in open capillaries on a Gallenkamp apparatus and are uncorrected. Merck silica gel 60 (230–400 mesh) was used for column chromatography. Merck TLC plates, silica gel 60 F₂₅₄, were used for

TLC. ¹H NMR spectra were recorded by means of a Bruker AC 200 or a Bruker DRX 400 AVANCE spectrometers in the indicated solvents (TMS as internal standard); the values of the chemical shifts are expressed in ppm, and the coupling constants (*J*) in Hz. Mass spectra were recorded on a ThermoFinnigan LCQ-Deca. The purity of compounds **10a–t** and **11a,b,e,g,n,q** was assessed by RP-HPLC by using two different eluent systems and was found to be higher than 98%. An Agilent 1100 series system equipped with a Zorbax Eclipse XDB-C8 (4.6 mm × 150 mm) column was used in the HPLC analysis with acetonitrile–water–methanol (60:35:5) or acetonitrile–methanol (70:30) as the mobile phase at a flow rate of 0.5 mL/min. UV detection was achieved at 254 nm.

N-Butyl-*N*-methyl-2-(4-methyl-3-oxo-2-phenyl-2,3-dihydro-1*H*-pyrazolo[3,4-*b*]quinolin-1-yl)acetamide (**10a**). A mixture of compound **13** (0.20 g, 0.73 mmol) in DMF (10 mL) with Na₂CO₃ (0.10 g, 0.94 mmol) was stirred at room temperature for 1 h. Then, a solution of bromoacetamide **16a** (0.31 g, 1.5 mmol) in DMF (3.0 mL) was added, and the resulting mixture was stirred overnight at room temperature. The reaction mixture was then concentrated under reduced pressure, and the residue was partitioned between dichloromethane and water. The organic layer was washed with water to neutrality, dried over sodium sulfate, and concentrated under reduced pressure. Purification of the residue by flash-chromatography with diethyl ether–ethyl acetate (8:2) as the eluent gave pure **10a** as a yellow crystalline solid (0.19 g, yield 65%, mp 133–134 °C). The ¹H NMR spectrum of this amide shows the presence of two different rotamers in equilibrium. For the sake of simplification, the integral intensities have not been given. ¹H NMR (200 MHz, CDCl₃): 0.76 (m), 0.94–1.38 (m), 2.65 (s), 2.73 (s), 2.97–3.09 (m), 3.15 (s), 4.76 (s), 4.81 (s), 7.27 (m), 7.38–7.68 (m), 7.71 (m), 7.91 (d, *J* = 8.3), 8.08 (d, *J* = 8.4). MS (ESI): *m/z* 425 (*M* + Na⁺).

N-Butyl-*N*-methyl-2-(4-methyl-3-oxo-2-phenyl-2*H*-pyrazolo[3,4-*b*]quinolin-9(3*H*)-yl)acetamide (**11a**). The title compound was separated by flash chromatography [diethyl ether–ethyl acetate (8:2)] as the more polar fraction during the purification of isomer **10a**. Compound **11a** was further purified by precipitation with *n*-hexane from a dichloromethane solution to obtain a dark-red solid (0.045 g, yield 15%, mp 245–246 °C). The ¹H NMR spectrum of this amide shows the presence of two different rotamers in equilibrium. For the sake of simplification, the integral intensities have not been given. ¹H NMR (200Mz, CDCl₃): 0.89 (t, *J* = 7.2), 1.04 (t, *J* = 7.2), 1.24–1.82 (m), 2.99 (s), 3.04 (s), 3.21 (s), 3.39–3.52 (m), 5.18 (s), 5.23 (s), 7.13 (t, *J* = 7.4), 7.21–7.31 (m), 7.39 (t, *J* = 7.2), 7.64 (t, *J* = 7.7), 7.97 (d, *J* = 8.1), 8.17 (m). MS (ESI): *m/z* 425 (*M* + Na⁺).

Table 3. Effect of Compounds 10g,q,t in a Rat Model of Mononeuropathy (Right) Evaluated in the Paw Pressure Test^a

| compd | dose (mg/kg) po | | paw pressure (g) | | | |
|---------|-----------------|-------|------------------|-------------------------|-------------------------|-------------------------|
| | | | before treatment | after 15 min | after 30 min | after 45 min |
| 10g | 5 | left | 61.6 ± 2.5 | 57.8 ± 3.4 | 63.6 ± 2.8 | 61.4 ± 3.3 |
| | 5 | right | 32.5 ± 2.7 | 39.2 ± 2.7 | 35.9 ± 2.5 | 33.4 ± 2.8 |
| | 50 | left | 62.1 ± 2.4 | 61.0 ± 2.5 | 58.0 ± 2.0 | 59.0 ± 2.9 |
| | 50 | right | 34.0 ± 2.9 | 48.1 ± 3.2* | 44.0 ± 2.3 [^] | 37.0 ± 2.2 |
| 10q | 5 | left | 62.7 ± 2.3 | 58.7 ± 4.1 | 57.7 ± 3.8 | 64.1 ± 3.9 |
| | 5 | right | 33.1 ± 2.6 | 35.6 ± 3.5 | 36.4 ± 2.6 | 36.3 ± 3.7 |
| | 50 | left | 65.6 ± 2.2 | 60.7 ± 2.3 | 59.3 ± 1.8 | 63.1 ± 3.3 |
| | 50 | right | 32.5 ± 2.4 | 49.4 ± 2.8* | 47.2 ± 2.5* | 36.3 ± 2.6 |
| 10t | 5 | left | 58.9 ± 2.6 | 61.4 ± 3.5 | 58.4 ± 3.3 | 63.8 ± 3.2 |
| | 5 | right | 33.5 ± 3.2 | 44.8 ± 2.3 [^] | 35.8 ± 2.7 | 32.7 ± 2.8 |
| | 50 | left | 63.1 ± 2.6 | 62.2 ± 2.8 | 61.8 ± 3.2 | 64.8 ± 3.5 |
| | 50 | right | 31.8 ± 3.0 | 56.3 ± 2.2* | 49.4 ± 2.9* | 42.5 ± 2.5 [^] |
| vehicle | | left | 61.6 ± 2.7 | 63.5 ± 2.8 | 59.6 ± 2.6 | 63.0 ± 2.4 |
| | | right | 32.3 ± 2.5 | 34.8 ± 3.7 | 31.3 ± 2.8 | 32.9 ± 2.6 |

^a Each value is the mean ± SEM of at least 4–5 rats per group. [^]P < 0.05; *P < 0.01 versus vehicle-treated rats.

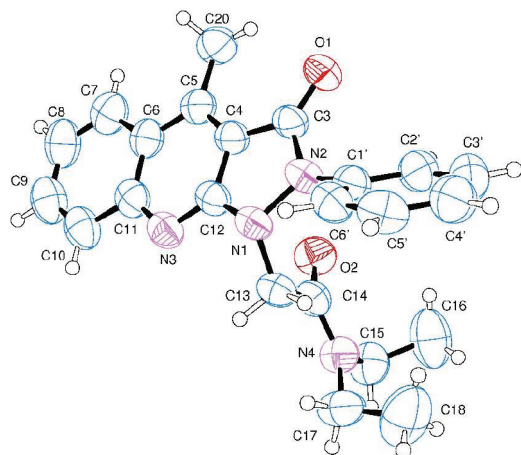


Figure 7. Crystallographic structure of compound 10b. Ellipsoids enclose 50% probability.

N,N-Diethyl-2-(4-methyl-3-oxo-2-phenyl-2,3-dihydro-1H-pyrazolo[3,4-*b*]quinolin-1-yl)acetamide (**10b**). The title compound was prepared from **13** (0.17 g, 0.62 mmol) and **16b** (0.31 g, 1.6 mmol) following the procedure described for compound **10a** and was purified by flash chromatography with diethyl ether–ethyl acetate (8:2) as the eluent to obtain a yellow crystalline solid (0.12 g, yield 50%) (Figure 7). An analytical sample was obtained by recrystallization from ethyl acetate by slow evaporation (mp 171–172 °C). ¹H NMR (200 MHz, CDCl₃): 0.82–0.94 (m, 6H), 2.97–3.20 (m, 7H), 4.78 (s, 2H), 7.28 (m, 1H), 7.38–7.60 (m, 5H), 7.70 (m, 1H), 7.92 (d, *J* = 8.7, 1H), 8.10 (d, *J* = 8.6, 1H). MS (ESI): 389 (M + H⁺).

N,N-Diethyl-2-(4-methyl-3-oxo-2-phenyl-2H-pyrazolo[3,4-*b*]quinolin-9(3H)-yl)acetamide (**11b**). The title compound was separated by flash chromatography [diethyl ether–ethyl acetate (8:2)] as the more polar fraction during the purification of isomer **10b**. Compound **11b** was further purified by washing with ethanol to obtain a dark-red solid (0.058 g, yield 24%, mp 260–261 °C). ¹H NMR (200 MHz, CDCl₃): 1.15 (t, *J* = 7.2, 3H), 1.37 (t, *J* = 7.0, 3H), 3.01 (s, 3H), 3.49 (m, 4H), 5.18 (s, 2H), 7.14 (t, *J* = 7.4, 1H), 7.23–7.30 (m, 2H), 7.39 (t, *J* = 7.8, 2H), 7.64 (t, *J* = 7.6, 1H), 7.95 (d, *J* = 8.0, 1H), 8.17 (d, *J* = 7.9, 2H). MS (ESI, negative ions): *m/z* 387 (M – H⁺).

N,N-Diisopropyl-2-(4-methyl-3-oxo-2-phenyl-2,3-dihydro-1H-pyrazolo[3,4-*b*]quinolin-1-yl)acetamide (**10c**). The title compound was prepared from **13** (0.15 g, 0.54 mmol) and **16c** (0.25 g, 1.1 mmol) following the procedure described for compound **10a** and was purified by flash chromatography with *n*-hexane–ethyl acetate (65:35) as the eluent to obtain a yellow crystalline solid (0.056 g, yield 25%). An analytical sample was obtained by recrystallization from ethyl acetate by slow evaporation (mp 215–216 °C). ¹H NMR (200 MHz, CDCl₃): 0.91 (d, *J* = 6.2, 6H), 1.10 (d, *J* = 6.2, 6H), 3.17 (s, 3H), 3.37 (m, 1H), 3.62 (m, 1H), 4.78 (s, 2H), 7.29 (m, 1H), 7.40–7.56 (m, 5H), 7.70 (m, 1H), 7.92 (d, *J* = 8.7, 1H), 8.10 (d, *J* = 8.8, 1H). MS (ESI): *m/z* 417 (M + H⁺).

N,N-Dipropyl-2-(4-methyl-3-oxo-2-phenyl-2,3-dihydro-1H-pyrazolo[3,4-*b*]quinolin-1-yl)-acetamide (**10d**). The title compound was prepared from **13** (0.15 g, 0.54 mmol) and **16d** (0.25 g, 1.1 mmol) following the procedure described for compound **10a** and was purified by flash chromatography with *n*-hexane–ethyl acetate (65:35) as the eluent to obtain a yellow oil which crystallized on standing (0.090 g, yield 40%, mp 141–142 °C). ¹H NMR (200 MHz, CDCl₃): 0.71 (m, 6H), 1.32 (m, 4H), 2.99 (m, 4H), 3.16 (s, 3H), 4.79 (s, 2H), 7.28 (m, 1H), 7.40–7.58 (m, 5H), 7.69 (t, *J* = 7.2, 1H), 7.91 (d, *J* = 8.5, 1H), 8.11 (d, *J* = 8.5, 1H). MS (ESI): *m/z* 417 (M + H⁺).

N,N-Dibutyl-2-(4-methyl-3-oxo-2-phenyl-2,3-dihydro-1H-pyrazolo[3,4-*b*]quinolin-1-yl)acetamide (**10e**). The title compound was prepared from **13** (0.15 g, 0.54 mmol) and **16e** (0.27 g, 1.1 mmol) following the procedure described for compound **10a** and was purified by flash chromatography with *n*-hexane–ethyl acetate (65:35) as the eluent to obtain a yellow crystalline solid (0.13 g, yield 54%) (Figure 8). An analytical sample was obtained by recrystallization from ethyl acetate by slow evaporation (mp 173–174 °C). ¹H NMR (200 MHz, CDCl₃): 0.74–0.85 (m, 6H), 1.02–1.37 (m, 8H), 2.92–3.10 (m, 4H), 3.17 (s, 3H), 4.80 (s, 2H), 7.30 (m, 1H), 7.40–7.59 (m, 5H), 7.70 (t, *J* = 8.0, 1H), 7.92 (d, *J* = 8.5, 1H), 8.12 (d, *J* = 8.2, 1H). MS (ESI): 445 (M + H⁺).

N,N-Dibutyl-2-(4-methyl-3-oxo-2-phenyl-2H-pyrazolo[3,4-*b*]quinolin-9(3H)-yl)acetamide (**11e**). The title compound was separated by flash chromatography [*n*-hexane–ethyl acetate (65:35)] as the more polar fraction during the purification of isomer **10e**. Compound **11e** was further purified by recrystallization from ethyl acetate to obtain a dark-red solid (0.052 g, yield 22%, mp 193–194 °C). ¹H NMR (200 MHz, CDCl₃): 0.88 (t, *J* = 7.1, 3H), 1.03 (t, *J* = 7.3, 3H), 1.19–1.84 (m, 8H), 3.04 (s, 3H), 3.33–3.50 (m, 4H), 5.23 (s, 2H), 7.13 (t, *J* = 7.4, 1H),

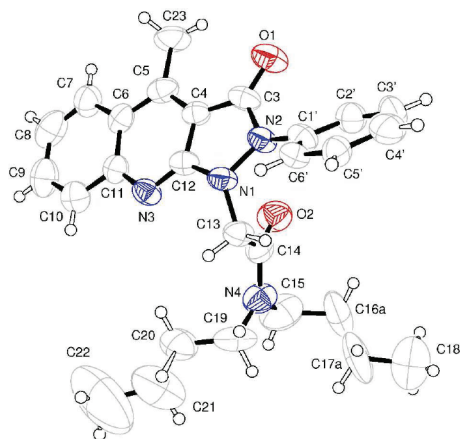


Figure 8. Crystallographic structure of compound **10e**. Ellipsoids enclose 50% probability.

7.22–7.42 (m, 4H), 7.65 (m, 1H), 7.97 (d, $J = 8.7$, 1H), 8.16 (d, $J = 8.2$, 2H). MS (ESI): 445 ($M + H^+$).

N-Methyl-2-(4-methyl-3-oxo-2-phenyl-2,3-dihydro-1H-pyrazolo[3,4-*b*]quinolin-1-yl)-*N*-phenylacetamide (**10f**). The title compound was prepared from **13** (0.10 g, 0.36 mmol) and **16f** (0.18 g, 0.79 mmol) following the procedure described for compound **10a** and was purified by flash chromatography with *n*-hexane–ethyl acetate (65:35) as the eluent to obtain a yellow crystalline solid (0.094 g, yield 62%, mp 209–210 °C). The ^1H NMR spectrum of this amide shows the presence of two different rotamers in equilibrium. For the sake of simplification, the integral intensities have not been given. ^1H NMR (200 MHz, CDCl_3): 3.03 (s, 3H), 3.18 (s, 3H), 4.52 (s, 2H), 6.75 (m, 2H), 7.26–7.53 (m, 9H), 7.73 (t, $J = 8.2$, 1H), 7.96 (d, $J = 8.0$, 1H), 8.13 (d, $J = 7.6$, 1H). MS (ESI): m/z 423 ($M + H^+$).

N-(4-Chlorophenyl)-*N*-methyl-2-(4-methyl-3-oxo-2-phenyl-2,3-dihydro-1H-pyrazolo[3,4-*b*]quinolin-1-yl)acetamide (**10g**). The title compound was prepared from **13** (0.10 g, 0.36 mmol) and **16g** (0.19 g, 0.72 mmol) following the procedure described for compound **10a** and was purified by flash chromatography with diethyl ether–ethyl acetate (7:3) as the eluent to obtain a yellow crystalline solid (0.086 g, yield 52%). An analytical sample was obtained by recrystallization from ethyl acetate by slow evaporation (mp 180–181 °C). ^1H NMR (200 MHz, CDCl_3): 3.01 (s, 3H), 3.18 (s, 3H), 4.52 (s, 2H), 6.70 (m, 2H), 7.22–7.37 (m, 3H), 7.43–7.54 (m, 5H), 7.73 (m, 1H), 7.95 (d, $J = 8.5$, 1H), 8.14 (d, $J = 8.7$, 1H). MS (ESI): m/z 457 ($M + H^+$).

N-(4-Chlorophenyl)-*N*-methyl-2-(4-methyl-3-oxo-2-phenyl-2H-pyrazolo[3,4-*b*]quinolin-9(3H)-yl)acetamide (**11g**). The title compound was separated by flash chromatography [diethyl ether–ethyl acetate (7:3)] as the more polar fraction during the purification of isomer **10g**. Compound **11g** was further purified by precipitation with *n*-hexane from a dichloromethane solution to obtain a dark-red solid (0.049 g, yield 30%, mp 239–240 °C). ^1H NMR (400 MHz, CDCl_3): 3.04 (s, 3H), 3.30 (s, 3H), 4.95 (s, 2H), 7.15–7.46 (m, 9H), 7.66 (t, $J = 7.8$, 1H), 7.97 (d, $J = 8.0$, 1H), 8.15 (d, $J = 7.8$, 2H). MS (ESI): m/z 479 ($M + \text{Na}^+$).

N-(4-Methoxyphenyl)-*N*-methyl-2-(4-methyl-3-oxo-2-phenyl-2,3-dihydro-1H-pyrazolo[3,4-*b*]quinolin-1-yl)acetamide (**10h**). The title compound was prepared from **13** (0.10 g, 0.36 mmol) and **16h** (0.19 g, 0.74 mmol) following the procedure described for compound **10a** and was purified by flash chromatography with acetate–petroleum ether (7:3) as the eluent to obtain a yellow crystalline solid (0.068 g, yield 42%). An analytical sample was obtained by recrystallization from ethyl acetate by slow evaporation (mp 205–207 °C). ^1H NMR (200 MHz, CDCl_3): 2.99 (s, 3H), 3.19 (s, 3H), 3.81 (s, 3H), 4.52 (s, 2H), 6.64–6.80

(m, 4H), 7.29–7.54 (m, 6H), 7.73 (m, 1H), 7.96 (d, $J = 8.4$, 1H), 8.14 (d, $J = 8.6$, 1H). MS (ESI): m/z 453 ($M + H^+$).

N-Benzyl-*N*-methyl-2-(4-methyl-3-oxo-2-phenyl-2,3-dihydro-1H-pyrazolo[3,4-*b*]quinolin-1-yl)acetamide (**10i**). The title compound was prepared from **13** (0.10 g, 0.36 mmol) and **16i** (0.18 g, 0.74 mmol) following the procedure described for compound **10a** and was purified by flash chromatography with *n*-hexane–ethyl acetate (65:35) as the eluent to obtain a yellow crystalline solid (0.097 g, yield 62%, mp 181–182 °C). The ^1H NMR spectrum of this amide shows the presence of two different rotamers in equilibrium. For the sake of simplification, the integral intensities have not been given. ^1H NMR (200 MHz, CDCl_3): 2.70 (s), 2.72 (s), 3.18 (s), 4.32 (s), 4.34 (s), 4.85 (s), 4.90 (s), 6.88 (m), 7.00 (m), 7.19–7.33 (m), 7.42–7.62 (m), 7.73 (t, $J = 7.5$), 7.95 (d, $J = 8.4$), 8.13 (d, $J = 8.4$). MS (ESI): m/z 437 ($M + H^+$).

N-Benzyl-*N*-ethyl-2-(4-methyl-3-oxo-2-phenyl-2,3-dihydro-1H-pyrazolo[3,4-*b*]quinolin-1-yl)acetamide (**10j**). The title compound was prepared from **13** (0.15 g, 0.54 mmol) and **16j** (0.29 g, 1.1 mmol) following the procedure described for compound **10a** and was purified by flash chromatography with *n*-hexane–ethyl acetate (65:35) as the eluent to obtain a yellow crystalline solid (0.11 g, yield 45%). An analytical sample was obtained by recrystallization from ethyl acetate by slow evaporation (mp 170–171 °C). The ^1H NMR spectrum of this amide shows the presence of two different rotamers in equilibrium. For the sake of simplification, the integral intensities have not been given. ^1H NMR (200 MHz, CDCl_3): 0.89 (m), 3.02–3.22 (m), 4.28 (s), 4.36 (s), 4.83 (s), 4.88 (s), 6.88 (m), 7.00 (m), 7.16–7.35 (m), 7.43–7.62 (m), 7.73 (t, $J = 7.0$), 7.95 (d, $J = 8.6$), 8.14 (d, $J = 8.1$). MS (ESI): m/z 451 ($M + H^+$).

N-Benzyl-*N*-isopropyl-2-(4-methyl-3-oxo-2-phenyl-2,3-dihydro-1H-pyrazolo[3,4-*b*]quinolin-1-yl)acetamide (**10k**). The title compound was prepared from **13** (0.15 g, 0.54 mmol) and **16k** (0.30 g, 1.1 mmol) following the procedure described for compound **10a** and was purified by flash chromatography with *n*-hexane–ethyl acetate (65:35) as the eluent to obtain a yellow crystalline solid (0.098 g, yield 39%). An analytical sample was obtained by recrystallization from ethyl acetate by slow evaporation (mp 156–157 °C). The ^1H NMR spectrum of this amide shows the presence of two different rotamers in equilibrium. For the sake of simplification, the integral intensities have not been given. ^1H NMR (200 MHz, CDCl_3): 0.92 (m), 3.18 (s), 3.96 (m), 4.20 (s), 4.34 (s), 4.51 (m), 4.70 (s), 4.97 (s), 6.92 (m), 7.10–7.34 (m), 7.42–7.57 (m), 7.73 (m), 7.95 (m), 8.13 (d, $J = 8.3$). MS (ESI): m/z 465 ($M + H^+$).

N-Benzyl-*N*-butyl-2-(4-methyl-3-oxo-2-phenyl-2,3-dihydro-1H-pyrazolo[3,4-*b*]quinolin-1-yl)acetamide (**10l**). The title compound was prepared from **13** (0.15 g, 0.54 mmol) and **16l** (0.31 g, 1.1 mmol) following the procedure described for compound **10a** and was purified by flash chromatography with *n*-hexane–ethyl acetate (65:35) as the eluent to obtain a yellow crystalline solid (0.083 g, yield 32%, mp 151–152 °C). The ^1H NMR spectrum of this amide shows the presence of two different rotamers in equilibrium. For the sake of simplification, the integral intensities have not been given. ^1H NMR (200 MHz, CDCl_3): 0.75 (m), 1.02–1.37 (m), 2.95 (t, $J = 7.2$), 3.10 (t, $J = 7.8$), 3.17 (s), 4.27 (s), 4.34 (s), 4.82 (s), 4.89 (s), 6.88 (m), 6.99 (m), 7.15–7.31 (m), 7.39–7.58 (m), 7.71 (t, $J = 7.8$), 7.95 (d, $J = 8.4$), 8.13 (d, $J = 8.2$). MS (ESI): m/z 479 ($M + H^+$).

N,N-Dibenzyl-2-(4-methyl-3-oxo-2-phenyl-2,3-dihydro-1H-pyrazolo[3,4-*b*]quinolin-1-yl)acetamide (**10m**). The title compound was prepared from **13** (0.15 g, 0.54 mmol) and **16m** (0.32 g, 1.1 mmol) following the procedure described for compound **10a** and was purified by flash chromatography with *n*-hexane–ethyl acetate (65:35) as the eluent to obtain a yellow crystalline solid (0.068 g, yield 25%). An analytical sample was obtained by recrystallization from ethyl acetate by slow evaporation (mp 185–187 °C). ^1H NMR (200 MHz, CDCl_3): 3.20 (s, 3H), 4.22 (s, 2H), 4.35 (s, 2H), 4.86 (s, 2H), 6.91 (m, 2H), 6.99 (m, 2H), 7.22–7.60 (m, 12H), 7.76 (t, $J = 7.7$, 1H), 7.97 (d, $J = 8.5$, 1H), 8.15 (d, $J = 8.3$, 1H). MS (ESI): m/z 513 ($M + H^+$).

N-Butyl-2-[2-(4-fluorophenyl)-4-methyl-3-oxo-2,3-dihydro-1H-pyrazolo[3,4-*b*]quinolin-1-yl]-*N*-methylacetamide (**10n**). The title compound was prepared from **14** (0.25 g, 0.85 mmol) and **16a** (0.38 g, 1.8 mmol) following the procedure described for compound **10a** and was purified by flash chromatography with diethyl ether–ethyl acetate (8:2) as the eluent to obtain a yellow crystalline solid (0.25 g, yield 70%). An analytical sample was obtained by recrystallization from ethyl acetate by slow evaporation (mp 161–162 °C). The ¹H NMR spectrum of this amide shows the presence of two different rotamers in equilibrium. For the sake of simplification, the integral intensities have not been given. ¹H NMR (200 MHz, CDCl₃): 0.75–0.87 (m), 1.01–1.38 (m), 2.70 (s), 2.82 (s), 3.05–3.13 (m), 3.16 (s), 4.73 (s), 4.79 (s), 7.18 (m), 7.42–7.58 (m), 7.72 (m), 7.92 (d, *J* = 8.5), 8.12 (d, *J* = 8.3). MS (ESI): *m/z* 421 (*M* + *H*⁺).

N-Butyl-2-[2-(4-fluorophenyl)-4-methyl-3-oxo-2H-pyrazolo[3,4-*b*]quinolin-9(3H)-yl]-*N*-methylacetamide (**11n**). The title compound was separated by flash chromatography [diethyl ether–ethyl acetate (8:2)] as the more polar fraction during the purification of isomer **10n**. Compound **11n** was further purified by washing with ethanol to obtain a dark-red solid (0.030 g, yield 8.4%, mp 259–260 °C). The ¹H NMR spectrum of this amide shows the presence of two different rotamers in equilibrium. For the sake of simplification, the integral intensities have not been given. ¹H NMR (200 MHz, CDCl₃): 0.88 (t, *J* = 7.3), 1.05 (t, *J* = 7.3), 1.23–1.83 (m), 2.99 (s), 3.04 (s), 3.22 (s), 3.39–3.52 (m), 5.20 (s), 5.23 (s), 7.07 (m), 7.20–7.32 (m), 7.65 (m), 7.98 (d, *J* = 7.7), 8.13 (m). MS (ESI): *m/z* 443 (*M* + *Na*⁺).

N,N-Diethyl-2-[2-(4-fluorophenyl)-4-methyl-3-oxo-2,3-dihydro-1H-pyrazolo[3,4-*b*]quinolin-1-yl]acetamide (**10o**). The title compound was prepared from **14** (0.25 g, 0.85 mmol) and **16b** (0.33 g, 1.7 mmol) following the procedure described for compound **10a** and was purified by flash chromatography with diethyl ether–ethyl acetate–dichloromethane (75:20:5) as the eluent to obtain a yellow crystalline solid (0.16 g, yield 46%). An analytical sample was obtained by recrystallization from ethyl acetate by slow evaporation (mp 225–226 °C). ¹H NMR (200 MHz, CDCl₃): 0.93 (t, *J* = 7.2, 6H), 3.04–3.20 (m, 7H), 4.80 (s, 2H), 7.18 (t, *J* = 8.6, 2H), 7.43–7.57 (m, 3H), 7.73 (t, *J* = 7.3, 1H), 7.96 (d, *J* = 8.5, 1H), 8.12 (d, *J* = 8.1, 1H). MS (ESI): *m/z* 407 (*M* + *H*⁺).

N,N-Dipropyl-2-[2-(4-fluorophenyl)-4-methyl-3-oxo-2,3-dihydro-1H-pyrazolo[3,4-*b*]quinolin-1-yl]acetamide (**10p**). The title compound was prepared from **14** (0.18 g, 0.61 mmol) and **16d** (0.29 g, 1.3 mmol) following the procedure described for compound **10a** and was purified by flash chromatography with *n*-hexane–ethyl acetate (65:35) as the eluent to obtain a yellow crystalline solid (0.144 g, yield 54%). An analytical sample was obtained by recrystallization from ethyl acetate by slow evaporation (mp 179–180 °C). ¹H NMR (CDCl₃): 0.66–0.80 (m, 6H), 1.34 (m, 4H), 3.01 (m, 4H), 3.16 (s, 3H), 4.77 (s, 2H), 7.18 (t, *J* = 8.4, 2H), 7.42–7.57 (m, 3H), 7.72 (t, *J* = 7.7, 1H), 7.92 (d, *J* = 8.4, 1H), 8.12 (d, *J* = 8.1, 1H). MS (ESI): *m/z* 435 (*M* + *H*⁺).

N-(4-Chlorophenyl)-2-[2-(4-fluorophenyl)-4-methyl-3-oxo-2,3-dihydro-1H-pyrazolo[3,4-*b*]quinolin-1-yl]-*N*-methylacetamide (**10q**). The title compound was prepared from **14** (0.20 g, 0.68 mmol) and **16g** (0.40 g, 1.5 mmol) following the procedure described for compound **10a** and was purified by flash chromatography with diethyl ether–ethyl acetate (7:3) as the eluent to obtain a yellow crystalline solid (0.20 g, yield 62%) (Figure 9). An analytical sample was obtained by recrystallization from ethyl acetate by slow evaporation (mp 199–200 °C). ¹H NMR (200 MHz, CDCl₃): 3.01 (s, 3H), 3.17 (s, 3H), 4.47 (s, 2H), 6.80 (d, *J* = 8.4, 2H), 7.13–7.17 (m, 2H), 7.30 (d, *J* = 8.5, 2H), 7.47 (m, 3H), 7.74 (t, *J* = 7.1, 1H), 7.95 (d, *J* = 8.5, 1H), 8.13 (d, *J* = 8.7, 1H). MS (ESI): *m/z* 475 (*M* + *H*⁺).

N-(4-Chlorophenyl)-2-[2-(4-fluorophenyl)-4-methyl-3-oxo-2H-pyrazolo[3,4-*b*]quinolin-9(3H)-yl]-*N*-methylacetamide (**11q**). The title compound was isolated by flash chromatography [diethyl ether–ethyl acetate (7:3)] as the more polar fraction during the purification of isomer **10q**. Compound **11q** was further purified by washing with ethanol to

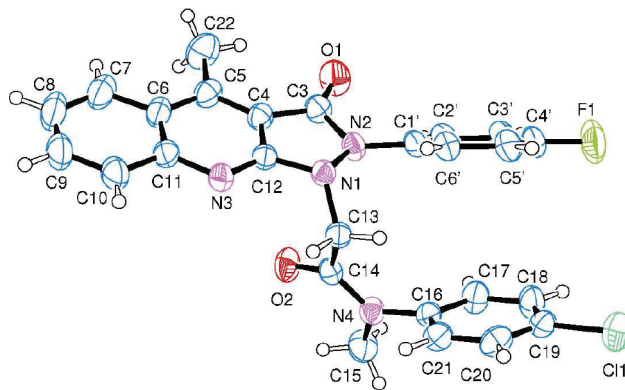


Figure 9. Crystallographic structure of compound **10q**. Ellipsoids enclose 50% probability.

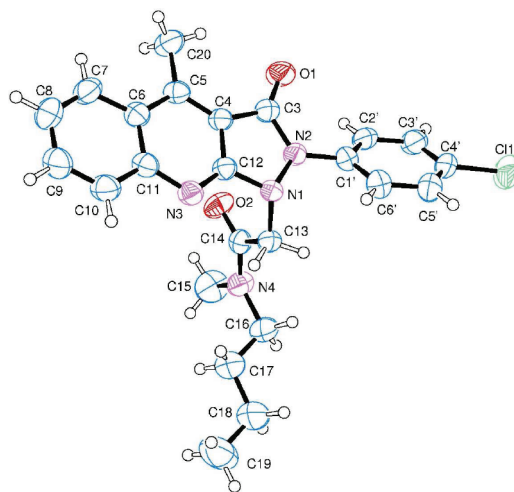


Figure 10. Crystallographic structure of compound **10r**. Ellipsoids enclose 50% probability.

obtain a dark-red solid (0.021 g, yield 6.5%, mp 232–234 °C). ¹H NMR (400 MHz, CDCl₃): 3.04 (s, 3H), 3.31 (s, 3H), 4.94 (s, 2H), 7.12 (t, *J* = 8.8, 2H), 7.19–7.36 (m, 4H), 7.46 (d, *J* = 8.3, 2H), 7.67 (t, *J* = 7.2, 1H), 7.98 (d, *J* = 7.2, 1H), 8.11 (m, 2H). MS (ESI): *m/z* 497 (*M* + *Na*⁺).

N-Butyl-2-[2-(4-chlorophenyl)-4-methyl-3-oxo-2,3-dihydro-1H-pyrazolo[3,4-*b*]quinolin-1-yl]-*N*-methylacetamide (**10r**). The title compound was prepared from **15** (0.20 g, 0.65 mmol) and **16a** (0.27 g, 1.3 mmol) following the procedure described for compound **10a** and was purified by flash chromatography with *n*-hexane–ethyl acetate (65:35) as the eluent to obtain a yellow crystalline solid (0.19 g, yield 67%) (Figure 10). An analytical sample was obtained by recrystallization from ethyl acetate by slow evaporation (mp 186–187 °C). The ¹H NMR spectrum of this amide shows the presence of two different rotamers in equilibrium. For the sake of simplification, the integral intensities have not been given. ¹H NMR (200 MHz, CDCl₃): 0.81 (m), 1.16 (m), 1.30 (m), 2.68 (s), 2.83 (s), 3.05–3.16 (m), 4.75 (s), 4.80 (s), 7.42–7.56 (m), 7.70 (m), 7.91 (d, *J* = 8.6), 8.12 (d, *J* = 8.0). MS (ESI): *m/z* 437 (*M* + *H*⁺).

2-[2-(4-Chlorophenyl)-4-methyl-3-oxo-2,3-dihydro-1H-pyrazolo[3,4-*b*]quinolin-1-yl]-*N,N*-dipropylacetamide (**10s**). The title compound was prepared from **15** (0.20 g, 0.65 mmol) and **16d** (0.29 g, 1.3 mmol) following the procedure described for compound **10a** and was purified by flash chromatography with *n*-hexane–ethyl acetate (65:35) as the eluent to obtain a yellow crystalline solid (0.154 g, yield 53%).

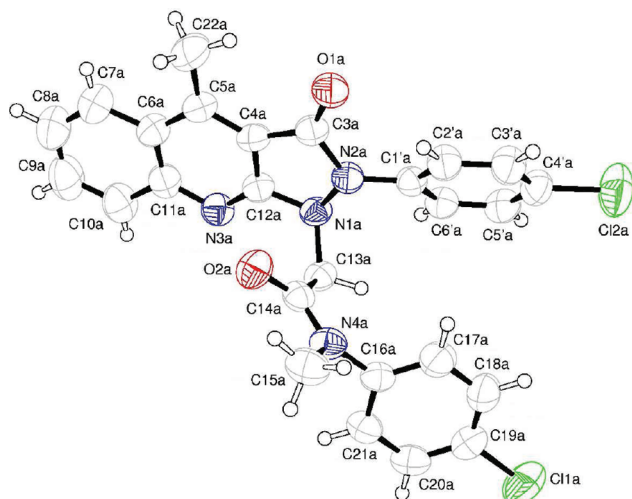


Figure 11. Crystallographic structure of compound **10t**. For clarity, only one molecule of the asymmetric unit is depicted. Ellipsoids enclose 50% probability.

An analytical sample was obtained by recrystallization from ethyl acetate by slow evaporation (mp 197–198 °C). ^1H NMR (200 MHz, CDCl_3): 0.71 (m, 6H), 1.32 (m, 4H), 2.99 (m, 4H), 3.12 (s, 3H), 4.76 (s, 2H), 7.38–7.54 (m, 5H), 7.68 (t, $J = 8.1$, 1H), 7.90 (d, $J = 8.2$, 1H), 8.07 (d, $J = 8.3$, 1H). MS (ESI): m/z 451 ($\text{M} + \text{H}^+$).

N-(4-Chlorophenyl)-2-[2-(4-chlorophenyl)-4-methyl-3-oxo-2,3-dihydro-1H-pyrazolo[3,4-*b*]quinolin-1-yl]-*N*-methylacetamide (**10t**). The title compound was prepared from **15** (0.20 g, 0.65 mmol) and **16g** (0.34 g, 1.3 mmol) following the procedure described for compound **10a** and was purified by flash chromatography with *n*-hexane–ethyl acetate (65:35) as the eluent to obtain a yellow crystalline solid (0.184 g, yield 58%) (Figure 11). An analytical sample was obtained by recrystallization from ethyl acetate by slow evaporation (mp 197–198 °C). ^1H NMR (200 MHz, CDCl_3): 3.01 (s, 3H), 3.17 (s, 3H), 4.50 (s, 2H), 6.79 (d, $J = 8.4$, 2H), 7.31 (d, $J = 8.3$, 2H), 7.48 (m, 5H), 7.76 (t, $J = 7.9$, 1H), 7.96 (d, $J = 8.6$, 1H), 8.14 (d, $J = 8.2$, 1H). MS (ESI): m/z 491 ($\text{M} + \text{H}^+$).

4-Methyl-2-phenyl-1H-pyrazolo[3,4-*b*]quinolin-3(2H)-one (**13**). A mixture of **12**¹⁴ (0.89 g, 3.56 mmol) in 20 mL of 1-pentanol with phenylhydrazine (1.4 mL, 14.2 mmol) was refluxed for 5 h. After cooling to room temperature, the precipitate was collected by filtration, washed with water, and dried under reduced pressure to give pure compound **13** as a dark solid (0.85 g, yield 87%, mp >300 °C dec). An analytical sample was obtained by recrystallization from CHCl_3 by slow evaporation. ^1H NMR ($\text{DMSO}-d_6$): 2.97 (s, 3H), 7.11 (t, $J = 7.3$, 1H), 7.24 (t, $J = 7.4$, 1H), 7.36–7.44 (m, 3H), 7.66 (t, $J = 7.3$, 1H), 8.00 (d, $J = 8.3$, 1H), 8.10 (d, $J = 8.1$, 2H), 12.61 (br s, 1H). MS (ESI): m/z 276 ($\text{M} + \text{H}^+$).

2-(4-Fluorophenyl)-4-methyl-1H-pyrazolo[3,4-*b*]quinolin-3(2H)-one (**14**). A mixture of **12**¹⁴ (1.2 g, 4.8 mmol) in 50 mL of 1-pentanol with (4-fluorophenyl)hydrazine hydrochloride (3.0 g, 18.5 mmol) and sodium carbonate (1.1 g, 10.4 mmol) was refluxed for 10 h. After cooling to room temperature, the precipitate was collected by filtration, washed with water, and dried under reduced pressure to give pure compound **14** as dark plates (1.3 g, yield 92%, mp >300 °C dec). ^1H NMR (200 MHz, $\text{DMSO}-d_6$): 2.98 (s, 3H), 7.25 (m, 3H), 7.43 (d, $J = 8.3$, 1H), 7.67 (t, $J = 7.6$, 1H), 8.01 (d, $J = 8.1$, 1H), 8.11 (m, 2H), 12.69 (br s, 1H). MS (ESI, negative ions): m/z 292 ($\text{M} - \text{H}^+$).

2-(4-Chlorophenyl)-4-methyl-1H-pyrazolo[3,4-*b*]quinolin-3(2H)-one (**15**). A mixture of **12**¹⁴ (1.1 g, 4.4 mmol) in 50 mL of 1-pentanol with (4-chlorophenyl)hydrazine hydrochloride (3.2 g, 18 mmol) and sodium carbonate (1.0 g, 9.4 mmol) was refluxed for 5 h. After cooling to room

temperature, the precipitate was collected by filtration, washed with water, and dried under reduced pressure to give pure compound **15** as dark-brown plates (1.1 g, yield 81%, mp >300 °C dec). ^1H NMR (200 MHz, $\text{DMSO}-d_6$): 2.98 (s, 3H), 7.25 (t, $J = 7.7$, 1H), 7.45 (m, 3H), 7.67 (t, $J = 7.6$, 1H), 8.01 (d, $J = 8.3$, 1H), 8.14 (d, $J = 8.8$, 2H), 12.69 (br s, 1H). MS (ESI, negative ions): m/z 308 ($\text{M} - \text{H}^+$).

X-ray Crystallography. Single crystals of **10b,e,h,g,r,t** and **13** were submitted to X-ray data collection on an Oxford-Diffraction Xcalibur Sapphire 3 diffractometer with a graphite monochromated Mo $K\alpha$ radiation ($\lambda = 0.71073 \text{ \AA}$) at 293 K. The structures were solved by direct methods implemented in SHELXS-97 program.¹⁵ The refinements were carried out by full-matrix anisotropic least-squares on F^2 for all reflections for non-H atoms by means of the SHELXL-97 program.¹⁶ Crystallographic data (excluding structure factors) for the structures solved in this paper have been deposited with the Cambridge Crystallographic Data Centre as supplementary publication no. CCDC 817653, 817658, 817652, 817661, 817660, 817659, and 817651. Copies of the data can be obtained, free of charge, on application to CCDC, 12 Union Road, Cambridge CB2 1EZ, UK; (fax: +44 (0) 1223 336 033; or e-mail: deposit@ccdc.cam.ac.uk).

In Vitro Binding Assays. Male Sprague–Dawley CD rats (Charles River Italia, Calco, CO, Italy) with body masses of 200–250 g were used. Rats were acclimatized to the new housing conditions for at least one week. They were housed six per cage under an artificial 12 h light/12 h dark cycle (lights on at 08:00 h), a constant temperature of 22 ± 2 °C and a relative humidity of 65%. They had free access to water and standard laboratory food at all times. Animal care and handling throughout the experimental procedures were in accordance with the European Communities Council Directive of 24 November 1986 (86/609/EEC).

Rats were sacrificed by decapitation, their brains were rapidly dissected, and the cerebral cortex was immediately frozen on dry ice and stored at -80 °C until the assay was performed. The binding assays were performed as described in the literature.^{13b} On the day of the assay, the rat cerebral cortex was thawed and homogenized in 50 volumes of ice-cold Dulbecco's phosphate-buffered saline (PBS, pH 7.4) with a Polytron PT 10 homogenizer (setting 5 for 20 s). The homogenate was centrifuged at 40000g, 4 °C for 30 min; the resulting pellet was resuspended in the same volume of ice-cold buffer and recentrifuged. The new pellet was resuspended in 10 volumes of ice-cold incubation buffer (PBS) and used for the binding assay.

[^3H] **1** binding was measured in a final volume of 1000 μL , consisting of 100 μL of membrane suspension (0.15–0.20 mg of protein), 100 μL of [^3H] **1** (specific activity 83.4 Ci/mmol, New England Nuclear, Perkin-Elmer, Monza, MI, Italy; final assay concentration of 1 nM), 5 μL of drug solution or solvent (dimethyl sulfoxide), and 795 μL of PBS. The binding reaction was performed at 25 °C for 90 min and started with the addition of membranes. The incubation was terminated by rapid filtration through glass-fiber filters (Whatman GF/B, GE Healthcare, Milan, Italy) which had been presoaked with 0.3% polyethyleneimine and placed in a cell harvester filtration manifold (Brandel). The filters were washed five times with 4 mL of ice-cold PBS, and filter-bound radioactivity was quantified by liquid scintillation spectrometry. Non-specific binding was defined as binding in the presence of 10 μM of unlabeled compound **1** (Sigma-Aldrich, Milan, Italy). Specific binding was determined by subtracting the nonspecific from the total binding and was about 75–80% of the total binding. Sigmaplot 10 software (Systat Software, Inc., San Jose, CA, USA) was used to determine the concentration of the test compounds that inhibited [^3H]ligand binding by 50% (IC_{50}). Ten concentrations of each compound were assayed, each performed in duplicate.

In Vivo Studies. *Animals.* Male mice and rats from Harlan-Nossan (Comerio, Varese, Italy) breeding farm were used. Fifteen mice or four rats were housed per cage. The cages were placed in the experimental room 24 h before the test for acclimatization. The animals were kept at

23 ± 1 °C with a 12 h light/dark cycle, light at 7 a.m., with food and water ad libitum. All experiments were carried out according to the guidelines of the European Community Council.

Chronic Constriction Injury. A peripheral mononeuropathy was produced in adult rats by placing loosely constrictive ligatures around the common sciatic nerve according to the method described by Bennett.¹⁷ Rats were anaesthetised with chloral hydrate. The common sciatic nerve was exposed at the level of the middle of the thigh by blunt dissection through biceps femoris. Proximal to sciatica's trifurcation, about 1 cm of the nerve was freed of adhering tissue and four ligatures (3/0 silk tread) were tied loosely around it with about 1 mm spacing. The length of the nerve thus affected was 4–5 mm. Great care was taken to tie the ligatures so that the diameter of the nerve was seen to be just barely constricted when viewed with 40× magnification. In every animal, an identical dissection was performed on the opposite side except that the sciatic nerve was not ligated. The left paw was untouched.

Paw Pressure Test. The nociceptive threshold in the rat was determined with an analgesimeter (Ugo Basile, Varese, Italy) according to the method described by Leighton.¹⁸ The instrument exerts a force, which is applied at a constant rate (32 g per second) with a cone-shaped pusher on the upper surface of the rat hind paw. The force is continuously monitored by a pointer moving along a linear scale. The pain threshold is given by the force, which induces the first struggling movements from the rat. Pretested rats, which scored below 40 g or over 75 g during the test before drug administration (25%) were rejected. An arbitrary cut off value of 250 g was adopted.

Light/Dark Box Test. The apparatus (50 cm long, 20 cm wide, and 20 cm high) consisted of two equal acrylic compartments, one dark and one light, illuminated by a 60 W bulb lamp and separated by a divider with a 10 cm × 3 cm opening at floor level. Each mouse was tested by placing it in the center of the lighted area, away from the dark one, and allowing it to explore the novel environment for 5 min. The time spent in the illuminated side was measured. This test exploited the conflict between the animal's tendency to explore a new environment and its fear of bright light.¹⁹

Drugs. The new compounds and Emapunil were administered by the po route and were suspended in 1% carboxymethylcellulose (CMC) sodium salt and sonicated immediately before use. Drug concentrations were prepared in such a way that the necessary dose could be administered in a 10 mL/kg volume of carboxymethylcellulose 1% by the po route.

Statistical Analysis. All experimental result are given as the mean ± SEM. Each value represents the mean of 25 mice. An analysis of variance, ANOVA, followed by Fisher's protected least significant difference procedure for post hoc comparison, was used to verify significance between two means of behavioral results. The data were analyzed with the StatView software for Macintosh (1992). *P* values of less than 0.05 were considered significant.

Molecular Electrostatic Potential Calculations. For all compounds, the electrostatic potential was calculated by means of GAMESS and mapped onto the electron density surface. The electrostatic potential was computed using the Hartree–Fock functional and 6-31G* basis set. Results were visualized by means of MacMolplt program.

■ ASSOCIATED CONTENT

Supporting Information. Experimental details for the synthesis and the characterization of bromoacetamide intermediates **16a–m**. This material is available free of charge via the Internet at <http://pubs.acs.org>.

■ AUTHOR INFORMATION

Corresponding Author

*Phone: +39 0577 234320. Fax: +39 0577 234333. E-mail: cappelli@unisi.it.

■ ACKNOWLEDGMENT

We are grateful to Prof. Stefania D'Agata D'Ottavi for the careful reading of the manuscript and to Dr. Francesco Berrettini (CIADS, Università di Siena) for the X-ray data collection. This work was financially supported by Ministero dell'Istruzione, dell'Università e della Ricerca (MIUR)—Programmi di ricerca di Rilevante Interesse Nazionale (PRIN).

■ ABBREVIATIONS USED

TSPO, translocator protein (18 kDa); PBR, peripheral benzodiazepine receptor; CBR, central benzodiazepine receptor; VDAC, voltage-dependent anion channel; ANT, adenine nucleotide transporter; MPTP, mitochondrial permeability transition pore; PET, positron emission tomography; GABA, γ -aminobutyric acid; FRA, freely rotating aromatic ring; PAR, planar aromatic region; PBS, phosphate-buffered saline; CMC, carboxymethylcellulose

■ REFERENCES

- (1) Papadopoulos, V.; Baraldi, M.; Guilarte, T. R.; Knudsen, T. B.; Lacapère, J. J.; Lindemann, P.; Norenberg, M. D.; Nutt, D.; Weizman, A.; Zhang, M. R.; Gavish, M. Translocator protein (18 kDa): new nomenclature for the peripheral-type benzodiazepine receptor based on its structure and molecular function. *Trends Pharmacol. Sci.* **2006**, *27*, 402–409.
- (2) (a) Anholt, R.; Pedersen, P.; De Souza, E.; Snyder, S. The peripheral type benzodiazepine receptor. Localization to the mitochondrial outer membrane. *J. Biol. Chem.* **1986**, *261*, 576–583. (b) Lacapère, J.-J.; Papadopoulos, V. Peripheral-type benzodiazepine receptor: structure and function of a cholesterol-binding protein in steroid and bile acid biosynthesis. *Steroids* **2003**, *68*, 569–585.
- (3) Hardwick, M.; Fertikh, D.; Culty, M.; Li, H.; Vidic, B.; Papadopoulos, V. Peripheral-type benzodiazepine receptor (PBR) in human breast cancer: correlation of breast cancer cell aggressive phenotype with PBR expression, nuclear localization, and PBR-mediated cell proliferation and nuclear transport of cholesterol. *Cancer Res.* **1999**, *59*, 831–842.
- (4) Olson, J. M.; Ciliax, B. J.; Mancini, W. R.; Young, A. B. Presence of peripheral-type benzodiazepine binding sites on human erythrocyte membranes. *Eur. J. Pharmacol.* **1988**, *152*, 47–53.
- (5) (a) Veenman, L.; Papadopoulos, V.; Gavish, M. Channel-like functions of the 18 kDa translocator protein (TSPO): regulation of apoptosis and steroidogenesis as part of the host-defense response. *Curr. Pharm. Des.* **2007**, *13*, 2385–2405. (b) Veenman, L.; Gavish, M. The peripheral-type benzodiazepine receptor and the cardiovascular system. Implications for drug development. *Pharmacol. Ther.* **2006**, *110*, 503–524. (c) Papadopoulos, V.; Lecanu, L.; Brown, R. C.; Han, Z.; Yao, Z.-X. Peripheral-type benzodiazepine receptor in neurosteroid biosynthesis, neuropathology and neurological disorders. *Neuroscience* **2006**, *138*, 749–756. (d) Casellas, P.; Galiegue, S.; Basile, A. S. Peripheral benzodiazepine receptor and mitochondrial function. *Neurochem. Int.* **2002**, *40*, 475–486.
- (6) (a) Chen, M. K.; Guilarte, T. R. Translocator protein 18 kDa (TSPO): molecular sensor of brain injury and repair. *Pharmacol. Ther.* **2008**, *118*, 1–17. (b) Papadopoulos, V.; Lecanu, L. Translocator protein (18 kDa): an emerging therapeutic target in neurotrauma. *Exp. Neurol.* **2009**, *219*, 53–57.
- (7) (a) Gavish, M.; Bachman, I.; Shoukrun, R.; Katz, Y.; Veenman, L.; Weisinger, G.; Weizman, A. Enigma of the peripheral benzodiazepine receptor. *Pharmacol. Rev.* **1999**, *51*, 619–640. (b) Chelli, B.; Pini, S.; Abelli, M.; Cardini, A.; Lari, L.; Muti, M.; Gesi, C.; Cassano, G. B.; Lucacchini, A.; Martini, C. Platelet 18 kDa translocator protein density is reduced in depressed patients with adult separation anxiety. *Eur. Neuropsychopharmacol.* **2008**, *18*, 249–254. (c) Pini, S.; Martini, C.; Abelli, M.; Muti, M.; Gesi, C.; Montali, M.; Chelli, B.; Lucacchini, A.; Cassano, G. B. Peripheral-type benzodiazepine receptor binding sites in platelets of patients with panic disorder associated to separation anxiety symptoms. *Psychopharmacology* **2005**, *181*, 407–411.

- (8) (a) Romeo, E.; Auta, J.; Kozikowski, A. P.; Ma, D.; Papadopoulos, V.; Puia, G.; Costa, E.; Guidotti, A. 2-Aryl-3-indoleacetamides (FGIN-1): a new class of potent and specific ligands for the mitochondrial DBI receptor (MDR). *J. Pharmacol. Exp. Ther.* **1992**, *262*, 971–978. (b) Kozikowski, A. P.; Ma, D.; Brewer, J.; Sun, S.; Costa, E.; Romeo, E.; Guidotti, A. Chemistry, binding affinities, and behavioral properties of a new class of “antineophobic” mitochondrial DBI receptor complex (mDRC) ligands. *J. Med. Chem.* **1993**, *36*, 2908–2920.
- (9) Da Settimo, F.; Simorini, F.; Taliani, S.; La Motta, C.; Marini, A. M.; Salerno, S.; Bellandi, M.; Novellino, E.; Greco, G.; Cosimelli, B.; Da Pozzo, E.; Costa, B.; Simola, N.; Morelli, M.; Martini, C. Anxiolytic-like effects of *N,N*-dialkyl-2-phenylindol-3-ylglyoxylamides by modulation of translocator protein promoting neurosteroid biosynthesis. *J. Med. Chem.* **2008**, *51*, 5789–5797.
- (10) (a) Selleri, S.; Gratteri, P.; Costagli, C.; Bonaccini, C.; Costanzo, A.; Melani, F.; Guerrini, G.; Ciciani, G.; Costa, B.; Spinetti, F.; Martini, C.; Bruni, F. Insight into 2-phenylpyrazolo[1,5-*a*]pyrimidin-3-yl acetamides as peripheral benzodiazepine receptor ligands: synthesis, biological evaluation and 3D-QSAR investigation. *Bioorg. Med. Chem.* **2005**, *13*, 4821–4834.
- (11) (a) Ferzaz, B.; Brault, E.; Bourliaud, G.; Robert, J. P.; Poughon, G.; Claustre, Y.; Marguet, F.; Liere, P.; Schumacher, M.; Nowicki, J. P.; Fournier, J.; Marabout, B.; Sevrin, M.; George, P.; Soubrie, P.; Benavides, J.; Scatton, B. SSR180575 (7-chloro-*N,N*-5-trimethyl-4-oxo-3-phenyl-3,5-dihydro-4*H*-pyridazino[4,5-*b*]indole-1-acetamide), a peripheral benzodiazepine receptor ligand, promotes neuronal survival and repair. *J. Pharmacol. Exp. Ther.* **2002**, *301*, 1067–1078. (b) Vin, V.; Leducq, N.; Bono, F.; Herbert, J. M. Binding characteristics of SSR180575, a potent and selective peripheral benzodiazepine ligand. *Biochem. Biophys. Res. Commun.* **2003**, *310*, 785–790.
- (12) (a) Rupprecht, R.; Rammes, G.; Eser, D.; Baghai, T. C.; Schulle, C.; Nothdurfter, C.; Troxler, T.; Gentsch, C.; Kalkman, H. O.; Chaperon, F.; Uzunov, V.; McAllister, K.; Bertaina-Anglade, V.; Drieu La Rochelle, C.; Tuerck, D.; Floesser, A.; Kiese, B.; Schumacher, M.; Landgraf, R.; Holsboer, F.; Kucher, K. Translocator protein (18 kD) as target for anxiolytics without benzodiazepine-like side effects. *Science* **2009**, *325*, 490–493. (b) Kita, A.; Kohayakawa, H.; Kinoshita, T.; Ochi, Y.; Nakamichi, K.; Kurumiya, S.; Furukawa, K.; Oka, M. Antianxiety and antidepressant-like effects of AC-5216, a novel mitochondrial benzodiazepine receptor ligand. *Br. J. Pharmacol.* **2004**, *142*, 1059–1072.
- (13) (a) Anzini, M.; Cappelli, A.; Vomero, S.; Giorgi, G.; Langer, T.; Bruni, G.; Romeo, M. R.; Basile, A. S. Molecular basis of peripheral vs central benzodiazepine receptor selectivity in a new class of peripheral benzodiazepine receptor ligands related to alpidem. *J. Med. Chem.* **1996**, *39*, 4275–4284. (b) Cappelli, A.; Giuliani, G.; Valenti, S.; Anzini, M.; Vomero, S.; Giorgi, G.; Sogliano, C.; Maciocco, E.; Biggio, G.; Concas, A. Synthesis and structure–activity relationship studies in peripheral benzodiazepine receptor ligands related to alpidem. *Bioorg. Med. Chem.* **2008**, *16*, 3428–3437.
- (14) Cappelli, A.; Anzini, M.; Vomero, S.; Mennuni, L.; Makovec, F.; Doucet, E.; Hamon, M.; Menziani, M. C.; De Benedetti, P. G.; Giorgi, G.; Ghelardini, C.; Collina, S. Novel potent 5-HT₃ receptor ligands based on the pyrrolidone structure: synthesis, biological evaluation, and computational rationalization of the ligand-receptor interaction modalities. *Bioorg. Med. Chem.* **2002**, *10*, 779–801.
- (15) Sheldrick, G. M. *SHELXS-97, Release 97–2, A Program for Automatic Solution of Crystal Structures*; University of Göttingen: Göttingen, Germany, 1997.
- (16) Sheldrick, G. M. *SHELXL-97, Release 97–2, A Program for Crystal Structure Refinement*; University of Göttingen: Göttingen, Germany, 1997.
- (17) Bennett, G. J.; Xie, Y. K. A peripheral mononeuropathy in rat that produces disorders of pain sensation like those seen in man. *Pain* **1988**, *33*, 87–107.
- (18) Leighton, G. E.; Rodriguez, R. E.; Hill, R. G.; Hughes, J. kappa-Opioid agonists produce antinociception after iv and icv but not intrathecal administration in the rat. *Br. J. Pharmacol.* **1988**, *93*, 553–560.
- (19) Walsh, D. M.; Stratton, S. C.; Harvey, F. J.; Beresford, I. J.; Hagan, R. M. The anxiolytic-like activity of GR159897, a non-peptide NK₂ receptor antagonist, in rodent and primate models of anxiety. *Psychopharmacology* **1995**, *122*, 186–191.